

Reaction Monitoring of Cementing Materials through Multivariate Techniques Applied to time-resolved Synchrotron X-Ray Diffraction Data

Alessandra Taris^{*a}, Massimiliano Grosso^a, Alberto Viani^c, Mariarosa Brundu^b, Vincenzo Guida^b

^aDipartimento di Ingegneria Meccanica, Chimica e dei Materiali, Università degli Studi di Cagliari, Via Marengo 2, Cagliari 09123, Italy

^bProcter & Gamble, Pomezia R&D Research Center, Via Ardeatina 100, Pomezia 00040, Italy

^cInstitute of Theoretical and Applied Mechanics ASCR, Centre of Excellence Telč, Batelovská 485, Telč CZ- 58856, Czech Republic

a.taris@dimcm.unica.it

In this work, the setting reaction of magnesium potassium phosphate ceramic (MKPC) from magnesia (MgO) and potassium di-hydrogen phosphate was investigated by means of in-situ synchrotron X-ray powder diffraction (XRPD). The experimental data were analyzed through multivariate statistical techniques that enabled a real time and reliable understanding of the phenomena occurring in the process. Here, a method combining Multivariate Curve Resolution - Alternating Least Squares (MCR-ALS) with Evolving Factor Analysis (EFA) was proposed. Comparison with the conventional methods showed that the compounds involved in the process can be correctly distinguished and the main reaction steps, such as reactants consumption, occurrence of intermediate amorphous phase and MKPC formation can be clearly identified.

1. Introduction

MKPC is a chemically-bonded ceramic (Wagh, 2004) attractive for applications like waste encapsulation, bone repair, natural fibre composites. When MgO reacts with potassium di-hydrogen phosphate (KDP) in solution, formation of K-struvite (MKP) occurs: $\text{MgO} + \text{KH}_2\text{PO}_4 + 5\text{H}_2\text{O} = \text{MgKPO}_4 \cdot 6\text{H}_2\text{O}$. Several mechanisms for this reaction have been proposed, but kinetic studies are scarce and none of them provided quantitative data (Ding et al., 2012). Moreover, there are experimental evidences that, besides crystalline MKP, an amorphous phase also forms which can be considered as a precursor of the crystalline MKP. Over long times, it has been found that its amount decreases whereas that of crystalline MKP increases. This leads to an improvement of the final product mechanical properties (Viani et al., 2014). At the current state of knowledge, the nature of this amorphous phase remains unexplained. Recent kinetic synchrotron diffraction experiments allowed for the description of the reaction as being initially driven by the dissolution of MgO in aqueous solution to form an intermediate product accumulating at the grain surface. This thickening layer hindered further diffusion of water shifting the mechanism towards a diffusion controlled one. Although, the theoretical molar ratio of magnesium to phosphate should be stoichiometric, it was observed that in the final product, residual reactants might be however present. This phenomenon could be due to: (i) low solubility of MgO and (ii) mass transfer resistance of others reactants through the product and intermediate species that accumulate on magnesia grains surface. MKP crystallization reaction was modeled using an Avrami model followed by a first order chemical reaction, as water is available at the interface of the intermediate layer, and K^+ and PO_4^{3-} ions readily migrate through the open structure of elongated MKP crystals. Such interpretation should be supported by further evidence since, conventional analysis of X-rays diffraction (XRD) data allows for the evaluation of only the crystalline components. Therefore, since reaction mechanisms and physical phenomena are not

completely understood, monitoring the evolution of the system by means of complementary techniques has become essential for process understanding. Extracting useful information from XRD spectra is always extremely time consuming and, in case of wide-angle diffraction experiments, limited to the investigation of only the crystalline component. In this work, the MKPC formation was monitored by means of in-situ synchrotron X-Ray diffraction. Here, the application of Multivariate Curve Resolution – Alternating Least Square (MCR-ALS) combined with the Evolving Factory Analysis (EFA) algorithms to spectroscopic measurements, is reported. The goal is to investigate the reaction mechanisms and detect the different species, both crystalline and amorphous, involved in the reaction.

2. Experimental

2.1 Sample preparation

MgO powder obtained by calcination of MgCO_3 at 1400 °C was mixed with KDP by hand in agate mortar at unity molar ratio and then placed in a capillary 0.7 mm in diameter opened on both ends. The powder was laterally confined between 2 small layers of quartz wool, allowing for the water to flow through the capillary. The capillary was mounted on a goniometric head for data collection with one end connected to a vacuum pump. Water was introduced on the other end, but initially not in contact with the powders. After starting data collection, operating the vacuum pump, the water was gently allowed to flow through the capillary wetting the powder and defining the start of the experiment. The whole process was followed through a high resolution camera. The advantage of such experimental setup, described in more detail elsewhere (Conterosito et al. 2013), is that the reaction can be monitored from the very beginning. The downside was that no exact control on the water/solid ratio was possible.

2.2 XRPD measurements

Data were collected at 20 °C at the beamline BM01a, European Synchrotron Radiation Facility (ESRF), Grenoble (France), employing a wavelength of 0.6895 Å with the pilatus 2M detector (Dectris). The reaction was followed for 111.23 min collecting four scans/min allowing the capillary to swing on its axis of 60 °. Each spectrum was recorded covering a 2θ range 0.97 ° - 43.82 ° with a resolution of 0.0146 ° 2θ . Eventually, each spectrum $d_{(1 \times J)}^i$ recorded at the i -th time ($i = 1, \dots, I$) can be arranged into a matrix $D_{(I \times J)}$ representing the I experimental patterns collected at the different J diffraction angles 2θ .

3. Methods

The classical approach to the analysis of decomposition of the reactants and crystallization of MKP implies the integration of the area under Bragg reflection peaks obtained by the in situ synchrotron X-rays powder diffraction (XRPD) experiment for each one of the phases, normalization to phase fraction (α) and graphical representation α with respect to time. This procedure is time consuming, and is thus usually limited to only one peak for each phase. Furthermore, it requires preliminary knowledge of each powder pattern in order to exclude the overlap of peaks from different phases that otherwise adversely affects the kinetic interpretation. Here, the MCR-ALS approach is investigated as a viable alternative to the conventional one. Such technique decomposes the experimental $D_{(I \times J)}$ matrix in two matrices $C_{(I \times M)}$ and $S_{(M \times J)}^T$ (de Juan et al., 2009) as reported in equation (1).

$$D_{(I \times J)} = C_{(I \times M)} \cdot S_{(M \times J)}^T + E_{(I \times J)} \quad (1)$$

Equation (1) can be considered as the extension of the Lambert–Beer's law in matrix form: C is the estimated concentration profile for M components; S is the matrix representing the estimated spectra for the M components. MCR-ALS aims to find the matrices C and S which minimize the norm of the residual matrix E . This is accomplished with the Alternating Least Squares iterative optimization procedure starting from a suitable initial guess C^0 for C (or alternatively a feasible S^0 for S). During the ALS optimization, several (physical) constraints (e.g. non-negativity, unimodality, mass balance closure) should be applied in order to convey the algorithm towards the most proper estimation of the C and S profiles. A drawback of MCR-ALS is the lack of ability to separate compounds that behave together (kinetically) in the same manner (e.g. more reactants that decrease together over the time and/or unreacted compounds). As a consequence, the method does not lead to the detection of the actual chemicals but, in general, represents a mixture of the chemicals appearing in each estimated spectrum $s_{(1 \times J)}^m$ ($m=1, \dots, M$).

In order to improve the performance of the procedure for a more effective separation of the different real compounds in the system, a procedure was here proposed and briefly described below:

1. EFA algorithm was implemented in order to find the initial estimate C^0 of matrix C (De Juan et al., 2004);

2. MCR-ALS was performed and matrices C^1 and S^1 were computed.
3. A new initial guess S^{20} for the spectra matrix was calculated according to the steps:
 - 3.1. the matrix S^1 is decomposed taking into account the theoretical patterns available from database
 - 3.2. a baseline correction was applied on the resulting diffractograms;
4. The *pure compounds* diffractograms S^2 , were then estimated again with the MCR-ALS procedure by considering as the initial guess, the spectra matrix S^{20} previously obtained.

The procedure was implemented with a in-house written Matlab® code and MCR-ALS and EFA algorithms developed by Jaumot et al. (2005).

4. Results and discussion

4.1 Experimental spectra

By comparing XRPD patterns over the time with theoretical ones, three significant changes were identified (dissolution of reactants, amorphous phase formation and growth of MKP crystals) as depicted in Figure 1:

- a) at $t = 0$ the spectrum is characterized by a linear combination of the MgO and KDP patterns (Figure 1.a);
- b) at $t \approx 2.6$ min a change of the baseline is observed as broad peaks appear at 1.4 and $13^\circ 2\theta$ (Figure 1.b), probably due to the presence of an amorphous phase (see magnification of Figure 1.b on the right). In the meantime KDP and MgO begin to dissociate in solution;
- c) at $t \approx 5$ min, contribution of the KDP spectra disappears and only magnesia and amorphous phase are present (Figure 1.c);
- d) at $t \approx 15$ min MKP crystals start to grow (Figure 1.d);
- e) from $t \approx 30$ to 111 min (end of the experiment) spectra do not exhibit important changes (Figure 1.e). It should be noticed that MgO is not completely consumed since the reaction is controlled by diffusion as already mentioned in the introduction.

For our purposes, the subsequent analysis was limited to spectra collected from 0 to 35 min, where the most important changes were found to occur and data collected in the angular region $1-6^\circ 2\theta$ were removed because of the strong contribution coming from incoherent scattering from water. Thus the final data set will be arranged in a matrix $D_{(80 \times 1295)}$.

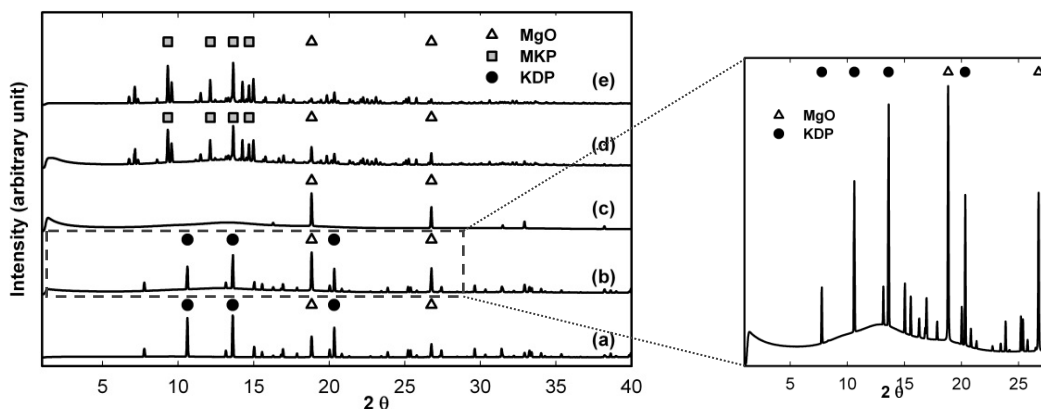


Figure 1. Representative raw spectra at different times with the main compounds patterns: (a) 0 min, (b) 2.6 min, (c) 5 min, (d) 15 min and (e) 30 min. Magnification of the spectrum (b) is depicted on the right.

4.2 Data processing

Data processing was performed according to the recipe introduced in section 3.

Step (1): initial estimate C^0 was calculated with the EFA algorithm. For the case at hand, since one main reaction takes place, only two components should be in principle identified (De Juan et al., 2004). However, occurrence of intermediate species would require the addition of more factors to describe appropriately the spectra time evolution. It was indeed found that the EFA results significantly improve when considering one intermediate species. On the other hand, choosing more than three factors did not lead to further improvements of the solution, which degenerate in the three factors case. Thus, one can conclude that EFA procedure clearly detects the existence of a unique intermediate component. In addition, three components adequately capture most of the variance of the matrix D and they might be reasonably associated to the

following three steps: (i) reactants consumption, (ii) development of intermediate species, (iii) product formation. The time evolution of the components estimated with the EFA procedure are reported in Figure 2;

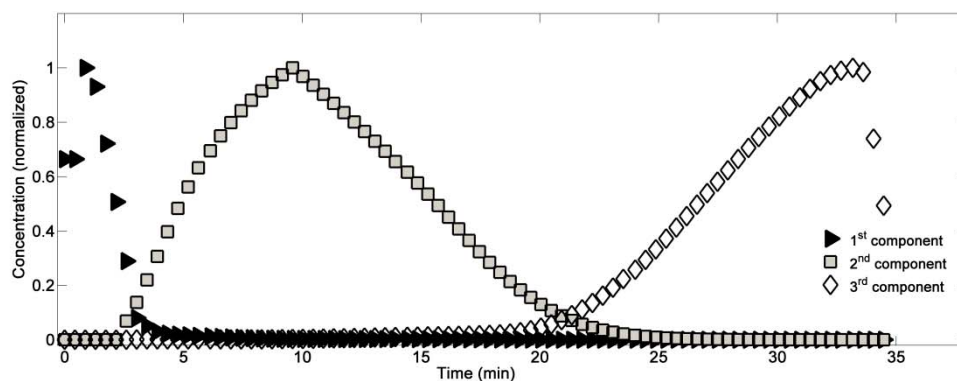


Figure 2. Concentration profiles estimated through EFA algorithm.

Step (2): matrices $C^1_{(80 \times 3)}$ and $S^1_{(1295 \times 3)}$ are then evaluated through the MCR-ALS algorithm and they are depicted in Figures 3 and 4, respectively. It is worthwhile noting that MCR-ALS algorithm provides an estimation of concentration profiles (see Figure 3 below) more plausible than the ones estimated with EFA (Figure 2): (i) the first component reasonably decreases after 3 min rather than starting from 0.8 and achieving a maximum value at 1 min; (ii) the intermediate species is constant (5-15 min) and then decreases; (iii) the third component increases after 15 min instead of 20 min.

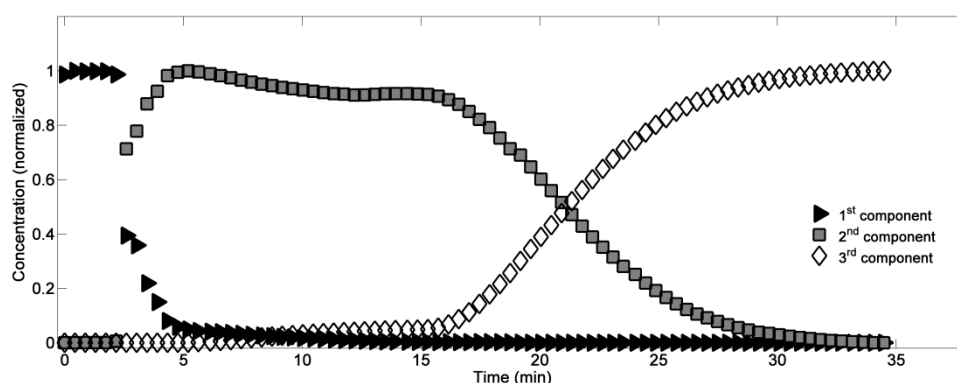


Figure 3. Concentration profiles C^1 estimated through MCR algorithm.

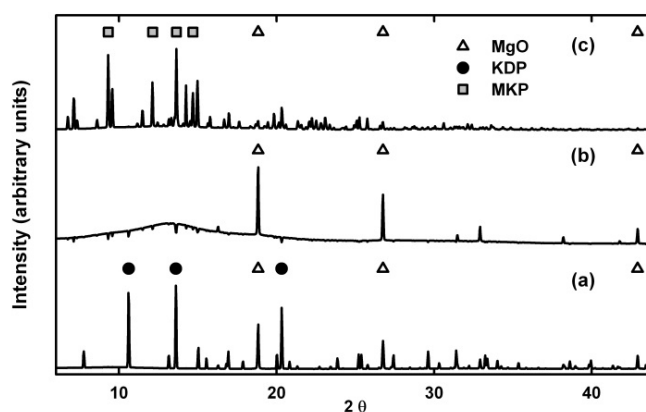


Figure 4. Evaluation of S^1 spectra estimated through MCR algorithm. White triangles, black circles and gray squares indicate MgO, KDP, MKP main patterns respectively

Figure 4 shows the three pseudo-spectra S^1 estimated with MCR-ALS along with the main patterns of the pure compounds MgO, KDP and MKP. It appears that they may be associated to: (a) MgO plus KDP; (b) MgO and an undefined intermediate species (likely corresponding to the amorphous phase); (c) MKP and MgO.

Step (3): As already reported, MgO contribution was present in all the S^1 spectra, since it does not react completely. This feature may degrade the effectiveness of the MCR-ALS procedure, and for this reason the protocol requires further refinements. The goal is to remove from the analysis the interference coming from unreacted species (for the case at hand MgO). Then, the contribution of the unreacted MgO diffractogram d_{MgO} observed at the end of the experiment was subtracted from the raw matrix D . Thus a new data set D^R was calculated with $d^R_i = d_i - d_{MgO}$ ($i=1, \dots, 80$) and unreacted species were filtered out from the analysis.

Then, the S^{20} matrix was determined by splitting the first spectrum (Figure 4.a) into two contributions pertaining the MgO and KDP through comparison with the theoretical patterns and removing the MgO patterns from the other spectra of S^1 (see Figure 4.b and 4.c). Eventually, four compounds spectra were determined and arranged in the matrix S^{20} .

The matrix D^R and S^{20} are then used as input in the MCR-ALS that provides the estimation of the spectra S^2 and C^2 . Then, the unreacted concentration of MgO, predicted through equation (2), was eventually added to the MgO concentration.

$$c_{MgO} = d_{MgO} \cdot (S^{2T})^+ \quad (2)$$

Where c_{MgO} is the predicted concentration of MgO unreacted and $(S^{2T})^+$ is the pseudo-inverse of S^2 .

Step (4): Figure 5 shows the estimated S^2 spectra together with the main theoretical patterns of the MgO, KDP and MKP. It can be concluded that the first three estimated spectra agree very well with the theoretical patterns of MgO (Figure 5.a), KDP (Figure 5.b) and MKP (Figure 5.c). In addition a spectrum for the intermediate phase is also provided (Figure 5.d). Although a perfect separation among the compounds spectra had not been achieved, the refinement here proposed greatly improves the following estimation of concentration profiles.

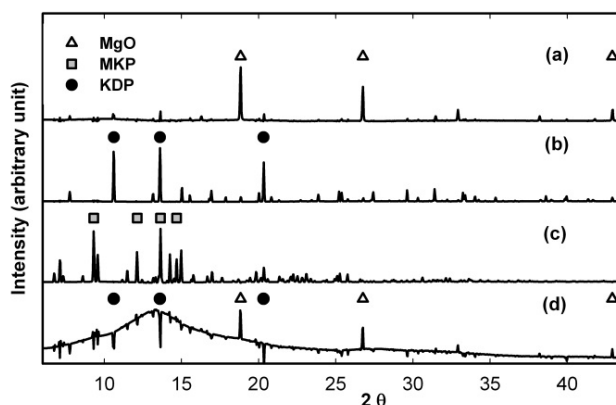


Figure 5. Evaluation of S^2 spectra.

Figure 6 shows the concentrations c_m^2 ($m=1, \dots, 4$) calculated with the proposed procedure and normalized with respect to its maximum value. Moreover, the α conversion values obtained from the conventional kinetic analysis (Banford et al., 1980) are also reported for sake of comparison. A really good agreement between the concentration profiles estimated with the MCR-ALS procedure and the conventional one was appreciated. It is worth noting that MCR-ALS provides an additional fourth component, whose contribution is considered to be due to the non-crystalline fraction. Its behaviour is coherent with previous observations showing a quick formation of an amorphous fraction at the initial stage of the reaction with its subsequent conversion into crystalline MKP (Viani et al., 2014). A reliable description of reaction dynamics was achieved. In fact, according to spectra analysis in section 4.1, five regions can be identified in Figure 6:

1. $t= 0 \div 2.6$ min: MgO and KDP are at the maximum values, while the amorphous phase starts from value greater than zero, likely due to the water scattering;
2. $t=2.6 \div 5$ min: KDP rapidly disappears as dissolves in solution, meanwhile the amorphous phase quickly increases reaching its maximum;
3. $t=5 \div 15$ min: amorphous phase concentration stays constant, in the meantime MgO keeps dissolving in solution;

4. $t=15\pm 30$ min: at $t=15$ min the onset of MKP crystallization and decrease of the amorphous phase are evident;
5. $t>30$ min: a flattening out of the amorphous decay and crystal growth rate is observed and no significant changes in the system are appreciated. This is probably due to a change in mechanism or a diffusion barrier emerging as reaction progresses.

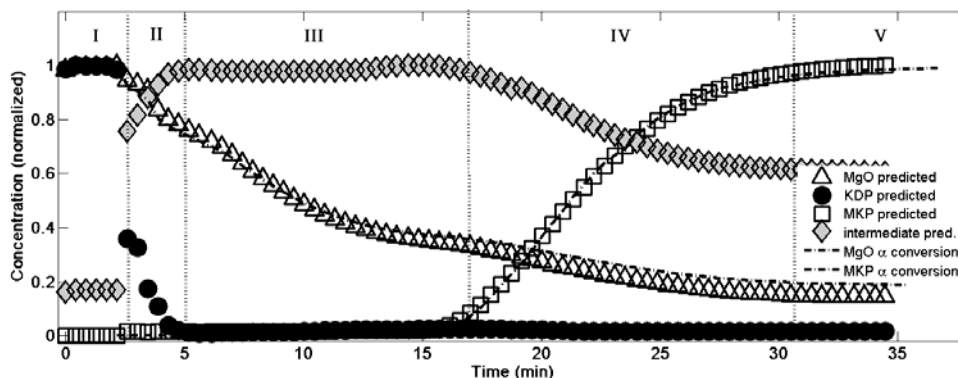


Figure 6. Normalized concentration profiles of MgO, KDP, MKP and the amorphous phase. Dashed and dashed-dotted lines represent the estimated α conversion of MKP and MgO, respectively

5. Conclusions

A procedure based on the MCR-ALS method combined with the EFA algorithm is here proposed in order to monitor the K-struvite formation through in situ x-ray diffraction measurements. The main benefits of the algorithm compared with the traditional analysis are summarized below: (i) it takes into account the whole diffraction angles rather than focusing on a limited number of peaks; (ii) it is less time consuming; (iii) it allows for the detection of the non-crystalline component that cannot be otherwise considered. The method here reported describes and identifies rather well the reaction mechanisms and it seems promising even for other applications involving the treatment of X-ray diffraction data.

References

- Bamford C.H., Tipper C.F.H., Eds., 1980. Comprehensive Chemical Kinetics, 22, 41-113. Elsevier, Amsterdam, the Netherlands.
- Conterosito E., Van Beek W., Palin L., Croce G., Perioli L., Viterbo D., 2013. Development of a fast and clean intercalation method for organic molecules into Layered Double Hydroxides. *Crystal Growth & Design*, 13(3), 1162-1169.
- de Juan A., Naveaa S., Diewokb J., Tauler R., 2004. Local rank exploratory analysis of evolving rank-deficient systems. *Chemometrics and Intelligent Laboratory Systems*, 70, 11 – 21.
- de Juan A., Rutan S.C., Tauler R., 2009. Two-Way Data Analysis: Multivariate Curve Resolution – Iterative Resolution Methods. *Comprehensive Chemometrics*, 2, 325-344, Eds. Brown S. D., Tauler R., Walczak B., Elsevier, Oxford, UK.
- Ding Z., Dong B., Xinga F., Hana N., Li Z., 2012. Cementing mechanism of potassium phosphate based magnesium phosphate cement. *Ceramics International*, 38, 6281–6288.
- Jaumot J., Gargallo R., de Juan A., Tauler R., 2005. A graphical user-friendly interface for MCR-ALS: a new tool for multivariate curve resolution in MATLAB. *Chemometrics and Intelligent Laboratory Systems*, 76(1), 101-110.
- Viani A., Gualtieri A. F., 2014. Preparation of magnesium phosphate cement by recycling the product of thermal transformation of asbestos containing wastes. *Cement and Concrete Research*, 58, 56–66.
- Wagh AS., 2004. Magnesium phosphate ceramics, in: E. Hurst, Ed., *Chemically bonded phosphate ceramics: 21st century materials with diverse applications*, Elsevier, Amsterdam, The Netherlands.